

THE AMERICAN MINERALOGIST

JOURNAL OF THE MINERALOGICAL SOCIETY OF AMERICA

Vol. 47

NOVEMBER-DECEMBER, 1962

Nos. 11 and 12

A NUCLEAR MAGNETIC RESONANCE DETERMINATION OF THE HYDROGEN POSITIONS IN $\text{Ca}(\text{OH})_2$ ¹

D. M. HENDERSON AND H. S. GUTOWSKY, *Department of Geology
and Noyes Chemical Laboratory, University of Illinois,
Urbana, Illinois.*

ABSTRACT

The structural locations of hydrogen in minerals and their artificial analogues are not readily obtainable by x -ray diffraction. This important structural feature, however, is particularly well adapted to investigation by a method based upon the phenomenon of nuclear magnetic resonance (nmr). Such an investigation was carried out on $\text{Ca}(\text{OH})_2$, a representative trioctahedral layer hydroxide, for which the proton magnetic resonance absorption was observed in crystal powders at liquid nitrogen and at room temperatures.

The broadening of the nmr absorption line by interactions among the magnetic nuclei can be measured as the second moment, ΔH_2^2 . A particular structural model can be tested by calculating the second moment for it and comparing the result with the experimental value. Measurement of the second moment for a crystal powder enables one structural parameter to be determined. In our study, the Bernal-Megaw model is assumed for the position of hydrogen in trioctahedral layer hydroxides; the parameter dealt with is a separation distance p which determines the amount of pucker in the hexagonal nets of hydrogen nuclei.

The experimental values obtained for the second moment are 12.4 ± 0.3 and 10.6 ± 0.7 gauss² at liquid nitrogen and room temperatures, respectively. The hydrogen positions obtained from the low-temperature data are given by $p = 0.62 \pm 0.04$ Å, which corresponds to $z_H = 0.437 \pm 0.004$ and an O-H distance of 0.99 ± 0.02 Å. The indicated errors are 95 per cent confidence limits. The smaller value of the second moment found at room temperature is due to the increased amplitudes of the proton motions and probably in part to a decrease in the effective O-H distance. In a brief discussion, these results are compared with related x -ray, neutron diffraction and infrared studies of $\text{Ca}(\text{OH})_2$ and an nmr study of brucite.

INTRODUCTION

Certain types of mineralogic structural information, such as the location of hydrogen, cannot be obtained readily by means of x -ray diffraction. Recently, methods of structural analysis have been developed which depend upon nuclear rather than electronic properties. One such method,

¹ A preliminary report of these results was presented at the 1956 annual meeting of the Mineralogical Society of America, Minneapolis (Henderson and Gutowsky, 1956; Gutowsky and Henderson, 1956).

based upon the phenomenon of nuclear magnetic resonance (nmr), is particularly useful for determining the structural position of hydrogen. The method may also be of value in providing information about such problems as: aluminum-silicon ordering in silicates, group reorientations, diffusion in solids, phase transitions, nature and behavior of water in hydrated crystals, and certain types of crystal imperfections. The necessary apparatus is becoming widely available, and interpretation of the experimental data is no more difficult than for single crystal x-ray work.

In the present paper we are concerned with applying nuclear magnetic resonance techniques to the determination of the hydrogen positions in the trioctahedral layer hydroxides. There are at least three such compounds which occur naturally: portlandite, $\text{Ca}(\text{OH})_2$; pyrochroite, $\text{Mn}(\text{OH})_2$; and brucite, $\text{Mg}(\text{OH})_2$. This mineral group is especially interesting because its structure persists as a major structural module in certain silicates such as the clays and micas.

Several structural studies have been made of these hydroxides, beginning with that of Aminoff (1919). However, at the time this work was started, only the positions of the heavier atoms, oxygen and metal, were known from x-ray diffraction studies (Wyckoff, 1948). In addition, Yeou Ta (1940) and Duval and Lecomte (1943) obtained evidence by means of infrared absorption that the O-H bond direction in brucite was oriented parallel to the *c* axis.

Although there was no direct evidence at the time as to the hydrogen positions in the trioctahedral layer hydroxides, Bernal and Megaw (1935) had made a reasonable prediction based on electrostatic and symmetric considerations. More recently, however, an infrared study of brucite by Mara and Sutherland (1953) cast some doubt about the hydrogen positions and upon the nature of the unit cell. For these reasons, as well as the fact that the proton has particularly good magnetic properties, $\text{Ca}(\text{OH})_2$ appeared to be a good candidate for study by proton magnetic resonance as presented below.

PRINCIPLES OF THE NMR METHOD

Inasmuch as magnetic resonance methods may be unfamiliar to many readers, a brief outline with references to the most pertinent literature will be presented before the experimental results and their analysis. Further details are available in general treatments of the subject such as those of Pake (1950) and of Andrew (1955).

The nmr phenomena result from the fact that, in addition to their more familiar properties of mass and electric charge, many nuclei have about them a weak magnetic field which can be described in terms of a

magnetic dipole moment \mathbf{u} . The origin of this field lies in the more or less complex circulation of the electric charges within the nucleus. This charge circulation is an electric current which generates the magnetic field. Also, the nucleus has an angular momentum \mathbf{p} or "spin" which results from the circulation of the mass associated with each element of electric charge.¹ Moreover, because of this association of mass and charge, there is a direct proportionality between \mathbf{p} and \mathbf{u} .

When a magnetic field \mathbf{H}_0 is applied to a magnetic nucleus, there is an interaction between them which tends to orient \mathbf{u} parallel to \mathbf{H}_0 , the interaction energy being given by $-\mu_H H_0$, where μ_H is the component of \mathbf{u} along \mathbf{H}_0 . However, quantum mechanical laws permit only certain orientations of \mathbf{u} with respect to \mathbf{H}_0 . In particular, p_H , the component of the angular momentum along \mathbf{H}_0 is restricted to discrete values of m equal to $I, I-1, \dots, -I$, in units of $h/2\pi$, where h is Planck's constant, I is the nuclear spin, and m is the nuclear magnetic quantum number. Thus, $Ih/2\pi$ is defined as the maximum value of p_H . It has been found that I may be integral or half-integral for a nucleus, depending upon its structure, and values as large as $9/2$ are not uncommon. The quantization of p_H leads to a corresponding quantization of μ_H and to the formation of a discrete set of nuclear magnetic energy levels,

$$E_m = -\mu_H H_0 = -mg\beta H_0, \quad (1)$$

where $g = \mu/I$ is the nuclear g -value and the proportionality constant β is the nuclear magneton which consists of several fundamental constants. In the expression for g , the nuclear magnetic moment μ is defined as the maximum value of μ_H , which is a constant characteristic of each nuclear species, as is I .

The set of energy levels described by Eq. (1) is similar to those giving rise to the Zeeman effect in atomic spectroscopy, except that the latter arises from the magnetic moment and spin of electrons. Moreover, as in the Zeeman effect, transitions can be induced among the energy levels, subject to the selection rule that $\Delta m = \pm 1$ and the presence of properly polarized radiation meeting the Bohr frequency condition, $\Delta E = h\nu$. Thus, the nuclei will absorb electromagnetic radiation when its frequency ν meets the condition

$$\nu_0 = \Delta E/h = g\beta H_0/h, \quad (2)$$

providing it is circularly polarized in the plane containing \mathbf{H}_0 . The values found for g are such that for typical magnetic fields of 5,000 to 15,000 gauss available in the laboratory for H_0 , the corresponding values of ν_0 lie generally in the 5 Mc/sec to 60 Mc/sec range. These frequencies are

¹ Vector quantities are given in bold-face type and magnitudes in lightface type.

in the radiofrequency region of the spectrum and the experimental methods for observing magnetic resonance spectra are radiofrequency in nature.

One severe limitation of nmr methods is that many nuclear species do not have suitable properties. For example, the even-even nuclei, those with an even number of neutrons and an even number of protons, have $I=0$ and a zero magnetic moment, so that they exhibit no nmr phenomena at all. Among such nuclei are C¹², O¹⁶, Mg²⁴, Si²⁸, S³², and Ca⁴⁰ as well as other important cases. This limitation is compensated for to some extent by the fact that nuclei with I greater than 1/2 have not only a magnetic dipole moment but also an electric quadrupole moment;

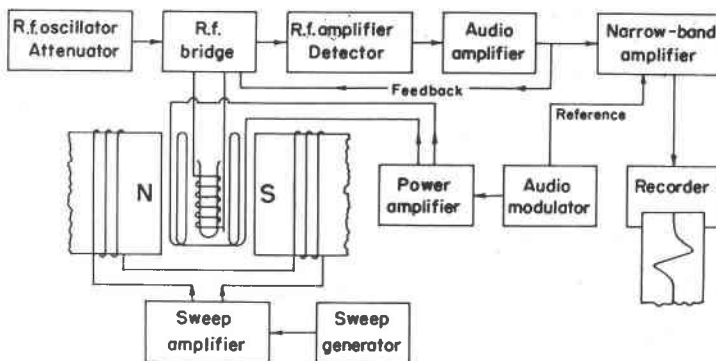


FIG. 1. Block diagram of a broad-line nmr spectrometer for structural studies of solids.

that is, instead of having spherical symmetry, the charge distribution within the nucleus is ellipsoidal in character. In consequence, besides magnetic effects there is an interaction of the nucleus with electric field gradients. The interactions can provide structural information, particularly on the distribution of electronic charge in ionic solids and in chemical bonds (Das and Hahn, 1958).

To return to nmr experiments, many types of apparatus have been used, depending in part upon the phenomena of interest. The block diagram in Fig. 1 is typical of the broad line spectrometers used for solid state structural studies. The energy source is a radiofrequency oscillator. The sample cell consists of a cylindrical coil of wire, mounted perpendicular to \mathbf{H}_0 in the gap of a magnet. The sample itself has a volume of the order of 1 cc and is contained ordinarily in a glass tube placed in the coil. The polarized radiation necessary to induce transitions in the nuclear magnetic energy is produced by an oscillating radiofrequency current in the coil, which is obtained by having the coil part of a tuned circuit coupled to the oscillator. A radio receiver amplifies and

detects the rf energy transmitted through the circuit containing the sample. The absorption spectrum can be traversed by keeping H_0 constant and sweeping the frequency of the rf oscillator, sample circuit, and receiver. The resonance absorption decreases the detected rf output, which is displayed on an oscilloscope, or recorded with a strip chart recorder.

In practice, however, as in our experiments and as shown in Fig. 1, it is often more convenient to keep the radiofrequency at a constant value, ν_0 , and to sweep the magnetic field through the resonance condition. The direct proportionality of ν_0 to H_0 in the resonance condition, Eq. (2), readily allows conversion of data from one basis to the other. Furthermore, in order to improve the sensitivity of the spectrometer, it is customary to use some device which makes the detected output of the receiver an audiofrequency rather than a direct current. This then permits the use of a sharply-tuned, low-noise audioamplifier after the receiver. Ordinarily, the audiofrequency nmr signal is obtained by modulating H_0 in the audiofrequency region with a set of auxiliary coils in the magnet. If an accurate plot of the line shape is desired, the amplitude of the field modulation is set at some fraction, about $\frac{1}{10}$, of the line width. H_0 is then swept slowly through the resonance condition, preferably linearly in time, to give a linear calibration of the recorder chart. The change in H_0 produced by its audiomodulation changes the amplitude of the resonance absorption and gives a corresponding modulation of the amplitude of the detected output from the receiver. The magnitude of this audiofrequency signal is proportional to the first derivative, with respect to H_0 , of the absorption line provided that the modulation of H_0 is a small enough fraction of the line width. The experimental curves obtained in our experiments are of this sort (Fig. 3).

Structural information is obtainable from the nmr absorption because the magnetic fields produced by the nuclear dipoles themselves effect the line shape. Consider a pair of identical nuclear magnetic moments μ separated by a distance r . The field H_0 at each nucleus is the sum of that applied by the external magnet, H_a , and a local field produced by the neighboring nucleus. Moreover, the sign of the local field depends on whether $m = +1/2$ or $-1/2$, for nuclei such as protons with $I=1/2$. In particular, one can write

$$H_0 = H_a + H_{1z} = H_a \pm \frac{3\mu}{2r^3} (3 \cos^2 \theta - 1), \quad (3)$$

where H_{1z} is the component of the local field along H_a , and θ is the angle between H_a and the internuclear vector. Therefore, for a single crystal consisting of isolated pairs of nuclei with the same θ and r , the nmr

absorption would be split into two components separated in gauss by $(3\mu/r^3)(3\cos^2\theta - 1)$. If the pairs are oriented at random as in a crystal powder, θ covers all values and a broadened doublet resonance results as shown by the dashed curve in Fig. 2a. In actual samples, such as hydrates, the magnetic dipole-dipole interactions between neighboring pairs are appreciable and this smooths out the absorption lines, as

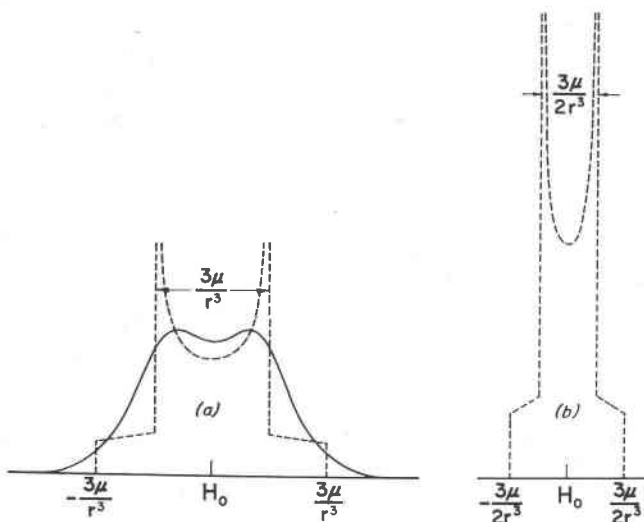


FIG. 2. The nmr absorption line shapes for nuclei with $I = \frac{1}{2}$, for a crystal powder in which the nuclei occur as pairs with an internuclear separation r . The dashed lines are theoretical curves which neglect the magnetic interactions between neighboring pairs. (a) This assumes that the nuclear positions are static, *i.e.* there are no vibrational or other "lattice" motions. The solid curve illustrates the broadening and smoothing-out effects of the magnetic interactions between neighboring pairs. (b) This shows the motional narrowing of the absorption to $\frac{1}{2}$ its "rigid lattice" width, which results from rotation of each pair about an axis perpendicular to its internuclear axis.

shown by the solid curve in Fig. 2a. Nonetheless, observation of the doublet splitting in a crystal powder can provide an accurate value for r ; and, for a single crystal, the angular dependence of the splitting gives in addition the orientation in the crystal of the internuclear vectors (Pake, 1948).

More often, as in $\text{Ca}(\text{OH})_2$, a nucleus will have several nearest neighbors rather than only one, and instead of a doublet line the nmr absorption is a broad, bell-shaped curve without resolved structure. In such cases, it is no longer feasible to relate the detailed line shape to the nuclear locations. However, the second moment, that is the mean square deviation, ΔH_z^2 , of the absorption intensity from the line center is

accessible easily from experiment. Moreover, it can be calculated readily (Van Vleck, 1948) for a single crystal from the structure of the solid by the equation

$$\Delta H_2^2(\text{calc}) = \frac{3}{2} \frac{I(I+1)}{N} g^2 \beta^2 \sum_{j < k} (3 \cos^2 \theta_{jk} - 1)^2 r_{jk}^{-6}, \quad (4)$$

where N is the number of nuclei in the "cell" over which the summation is taken. This summation converges rapidly; only neighbors within about 6 Å make significant contributions. In this equation, it is assumed that the only magnetic nuclei present in the sample are of the one species whose nmr absorption is observed; if there are other species present, another similar term for each must be added to Eq. (4).

As in the case of "isolated" nuclear pairs, the maximum amount of structural information is obtainable from the nmr absorption of a single crystal. However, the symmetry inherent in each space group restricts the amount of information available; nonetheless, a maximum of fifteen structural parameters is determinable from the angular dependence of the second moment for the nmr absorption of a particular set of nuclei (McCall and Hamming, 1959). Unfortunately, relatively large single crystals (1 to 2 cc) are needed for such studies.

For a crystal powder, with the crystallites randomly oriented, Eq. (4) must be averaged using the probability $\sin \theta d\theta$ of finding a given θ_{jk} . This gives

$$\Delta H_2^2(\text{calc}) = \frac{6}{5} \frac{I(I+1)}{N} \sum_{j < k} r_{jk}^{-6},$$

which, in cases where the magnetic nuclei occupy structurally equivalent sites, takes the simpler form

$$\Delta H_2^2(\text{calc}) = \frac{6}{5} \frac{I(I+1)}{2} \sum_k r_{jk}^{-6}. \quad (5)$$

Equation (5) provides one "bit" of information from which one structural feature can be established. However, this approach can still be very useful (Gutowsky *et al.*, 1949).

A final general point concerns the effects of nuclear motions. In the discussion above, it has been assumed that the internuclear distances r_{jk} and the angles θ_{jk} do not change with time, *i.e.* we are dealing with a "rigid lattice." This, of course, is an oversimplification in that at least zero point vibrational motions occur. Also, particularly in molecular crystals, it is not uncommon for group reorientations or diffusion to proceed at appreciable rates. In such cases, the static distances and angles of Eq. (4) must be replaced with the time dependent functions, $\theta_{jk}(t)$ and $r_{jk}(t)$, and an appropriate time average taken to determine

the apparent value of the second moment. These time averages reduce the second moment from the "rigid lattice" value. As an example, there is shown in Fig. 2b the partial narrowing of the nmr absorption by isolated nuclear pairs, which results from rotation of each pair about an axis perpendicular to its internuclear axis. The line width is reduced by a factor of $\frac{1}{2}$ and the second moment, $\frac{1}{4}$. Such motional narrowing must either be negligible or corrected for if Eqs. (4) and (5) are used for structural determination (Gutowsky *et al.*, 1954).

EXPERIMENTAL PROCEDURE AND RESULTS

Reagent $\text{Ca}(\text{OH})_2$ powder, the artificial analogue of portlandite, was chosen for study as best meeting the following compositional and crystallographic requirements or limitations. In contrast to mineral samples, its composition is that of the stoichiometric compound. It does not contain significant amounts of paramagnetic nuclear species other than hydrogen, or of undesirable paramagnetic atomic species. The required cell dimensions and position parameters for the heavier atoms are of better quality for $\text{Ca}(\text{OH})_2$ than for $\text{Mg}(\text{OH})_2$, because it tends to crystallize more perfectly. Crystal powder was used because sufficiently large single crystals were not available to us.

Recent studies of $\text{Ca}(\text{OH})_2$ and portlandite have been made by Swanson and Tatge (1953), Petch and Megaw (1954), Mara and Sutherland (1956), Busing and Levy (1957), Busing and Morgan (1958) and Petch (1961); earlier work is listed by Wyckoff (1948).

The samples consisted of approximately 1 g of "Baker Analyzed" reagent $\text{Ca}(\text{OH})_2$ powder which had been dried for a day at 100°C . and sealed in $2\frac{1}{2}$ inch lengths of $\frac{3}{8}$ inch O.D. soft glass tubing. The material was checked by the *x*-ray powder method to confirm that it (1) was the artificial analogue of portlandite, (2) contained no significant amounts of other phases, and (3) was well crystallized.

The proton absorption was observed for these samples using the broad-line nmr spectrometer and techniques described previously (Gutowsky, *et al.*, 1953). The essential features of the spectrometer are as indicated in Fig. 1. For the reasons outlined in the introductory section on nmr methods, the spectrometer records the first derivative of the absorption line as a function of the magnetic field applied. One of the experimental curves, obtained at a fixed radiofrequency of 26.84 Mc/sec by sweeping H_0 through a value of 6300 gauss, is reproduced in Fig. 3. In our experiments on $\text{Ca}(\text{OH})_2$, seven such curves were obtained at temperatures of 26° C . to 28° C . and thirteen in the interval of -196° C . to -185° C . The experiments at low temperature were performed to minimize line narrowing by thermal motions of the protons. Also, it was found that

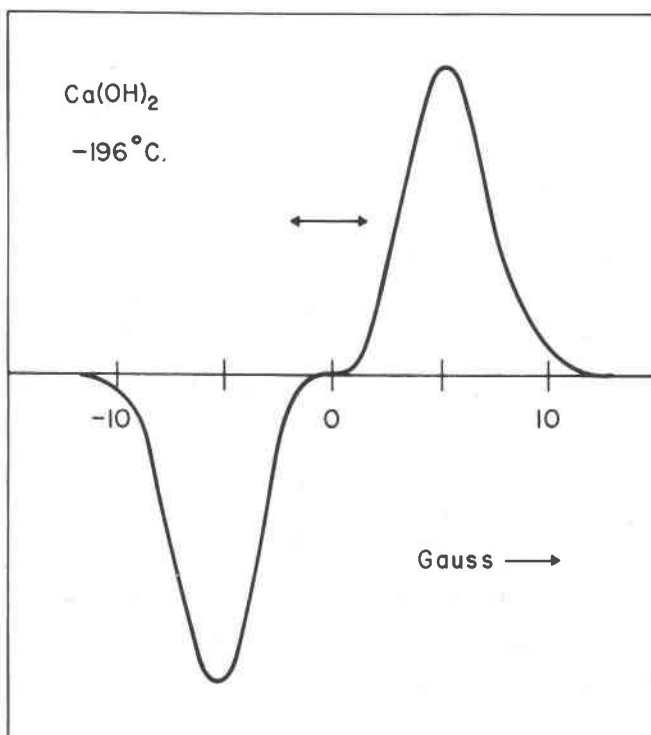


FIG. 3. The first derivative of the proton magnetic resonance absorption line, observed as a function of the applied magnetic field, for $\text{Ca}(\text{OH})_2$ powder at -196° C . and a fixed radiofrequency of 26.84 Mc/sec. The center of the absorption line corresponds to an applied field of about 6300 gauss; the arrow indicates the modulation amplitude.

spectra of better quality were obtained at liquid nitrogen temperatures.

In order to obtain structural information from the spectra we need the second moment of the absorption line for comparison with values calculated by the method of Van Vleck (1948) for various possible structures. In general, the second moment, m_2 , of a distribution is defined as

$$m_2 = \sum_i \phi_i (x_i - \bar{x})^2 / \sum_i \phi_i, \quad (6)$$

where ϕ_i is the frequency or probability of finding $x = x_i$. For a continuous function, centered at $x = 0$, the summations may be replaced by integrals to give

$$m_2 = \int_{-\infty}^{+\infty} x^2 f(x) dx / \int_{-\infty}^{+\infty} f(x) dx. \quad (7)$$

In the case of nmr absorption, the deviation $\Delta H = H_0 - H^*$ of the mag-

netic field from the center of the line corresponds to the variable x in Eq. (7), and the amplitude of the absorption is the function $f(x)$. Inasmuch as the experiment gives $f'(x)$, the first derivative of the absorption, it is preferable to recast Eq. (7) in terms of $f'(x)$. This gives

$$\Delta H_2^2(\text{obs}) = (1/3) \int_{-\infty}^{+\infty} x^3 f'(x) dx / \int_{-\infty}^{+\infty} x f'(x) dx. \quad (8)$$

Equation (8) was used to obtain $\Delta H_2^2(\text{obs})$ by numerical integration of the experimental curves for $f'(x)$. In turn these values were corrected for the broadening effects of modulating the magnetic field, by means of the relation derived by Andrew (1953), to give the experimental value

$$\Delta H_2^2(\text{exp}) = \Delta H_2^2(\text{obs}) - (1/4) H_m^2, \quad (9)$$

where H_m is the modulation amplitude in gauss. In this manner, a mean value of 12.4 gauss² with a standard deviation of 0.5 gauss² was obtained for $\Delta H_2^2(\text{exp})$ from the thirteen low temperature curves. A mean value of 10.6 gauss² with a standard deviation of 0.75 gauss² was obtained from the seven room temperature curves.

STRUCTURAL INTERPRETATION

As mentioned, the value of $\Delta H_2^2(\text{exp.})$ for the broadening of the resonance line by the dipolar interactions among the magnetic nuclei in a crystal powder enables one structural parameter to be determined. This is done by comparing $\Delta H_2^2(\text{exp.})$ with a theoretical $\Delta H_2^2(\text{calc.})$, obtained by means of Eq. (5) for a particular arrangement of magnetic nuclei.

For Ca(OH)₂, determination of the positions of the hydrogen nuclei required (1) knowledge about the positions of the heavy atoms by some other method, and (2) a model such that the proton positions are described by a single parameter of which the term $\sum r^{-6}$ in Eq. (5) is a sensitive function. The data required for condition (1) are listed in Table 1. They include the cell dimensions for a partly natural specimen of portlandite found in a long abandoned lime kiln (Megaw, 1933) and for fine-grained artificial material (Swanson and Tatge, 1953) similar to that used in this study.

The most reasonable proton arrangement, and one satisfying condition (2), is the one proposed by Bernal and Megaw (1935). Simple consideration of electostatics and symmetry indicated that, for space group $P\bar{3}m1$, the hydrogen nuclei probably are situated at the equivalent positions $\pm(\frac{1}{3}, \frac{2}{3}, z)$ having point symmetry $3m$. Moreover, they are so located that the value for z_H is in the interval $0.500 > z_H > z_0$, where $z_0 = 0.233$ (Petch, 1961).

The essential structural features are displayed in Fig. 4. It will be

TABLE I. STRUCTURAL DATA FOR $\text{Ca}(\text{OH})_2$ AND PORTLANDITE

Space group	$P\bar{3}m1$	$D3d\cdot3$	
Structure type	$C6$ (CdI_2 type)	$Z=1 \text{ Ca}(\text{OH})_2$	Ewald and Hermann (1931)
Atomic position parameters	Ca: 1 a 0, 0, 0 O: 2 d $\pm(\frac{1}{3}, \frac{2}{3}, z)$ O: $z_0 = 0.2330 \pm 0.0004$	pt. sym. $\bar{3}m$ pt. sym. $3m$	Wyckoff (1948) Petch (1961)
	H: 2 d $\pm(\frac{1}{3}, \frac{2}{3}, z)$ $0.500 > z_H > z_0$	pt. sym. $3m$	Bernal and Megaw (1935)
Cell dimensions	<i>Room Temp.</i> $a = 3.5925 \pm 0.0007 \text{ \AA}$ $c = 4.905 \pm 0.003 \text{ \AA}$ $c/a = 1.365$	-190° C.^2 $a = 3.585 \text{ \AA}$ $c = 4.871 \text{ \AA}$ $c/a = 1.359$	Megaw (1933) Portlandite from disused lime kiln
	27° C. $a = 3.593 \text{ \AA}$ $c = 4.909 \text{ \AA}$ $c/a = 1.366$	-190° C.^2 $a = 3.585 \text{ \AA}$ $c = 4.874 \text{ \AA}$ $c/a = 1.360$	Swanson and Tatge (1953) Artificial $\text{Ca}(\text{OH})_2$ powder

¹ Cell dimensions originally reported in kX have been recalculated to \AA .

² Cell dimensions listed for -190° C. have been calculated by means of the thermal expansion data of Megaw (1933).

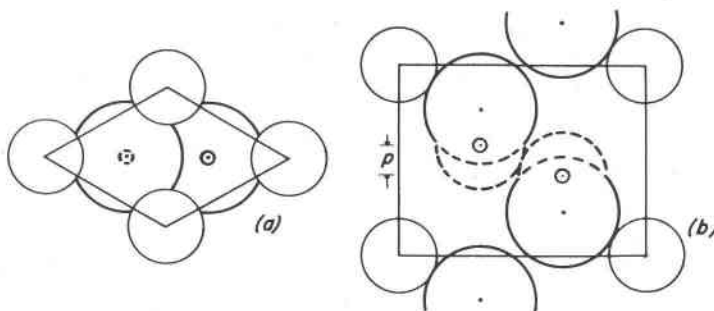


FIG. 4. The structure of portlandite, $\text{Ca}(\text{OH})_2$: (a) Plan view on (0001); (b) Section along (11-20) through center of cell; the symbol p designates the degree of pucker in the proton nets. Medium size circles centered on cell origins represent Ca atoms, large circles centered at $\pm(\frac{1}{3}, \frac{2}{3}, 0.233)$ represent oxygen atoms, and small heavy circles at $\pm(\frac{1}{3}, \frac{2}{3}, 0.43)$ represent hydrogen nuclei. The atomic radii shown are: $\text{Ca}^{2+} = 0.99 \text{ \AA}$, $\text{O}^{2-} = 1.40 \text{ \AA}$ and $\text{H} = 1.09 \text{ \AA}$ (one-half the distance H-H).

noted that the oxygen atoms occur in approximate hexagonal close packing. The individual layers have ideal planar close packing but equivalent layers are slightly contracted along c so that c/a is 1.366 rather than the ideal 1.633. Moreover, the individual layers are displaced along c so that adjacent layers are alternately slightly closer (2.286 Å at 25° C.) and slightly farther apart (2.620 Å at 25° C.) rather than equidistant. The calcium atoms occur in the sheets of octahedral sites between the closer pairs of oxygen layers; they are, in fact, responsible for this contraction. The hydrogen nuclei occur in puckered hexagonal nets centered on the planes between the more distant pairs of oxygen layers. In Fig. 5, it may be seen that the pucker of the hexagonal array of protons in each net converts it into two "sub-layers," which are equivalent and are separated by p , the single unknown parameter needed to fix the actual locations of the protons.

Because the second moment depends upon the inverse sixth power of the interproton distances, the summation $\sum_k r_{jk}^{-6}$ in Eq. (5) converges

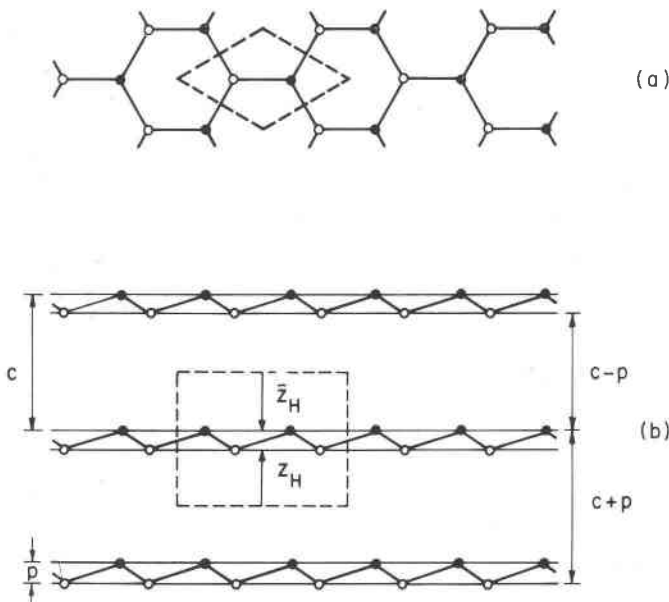


FIG. 5. The layer structure model for the distribution of hydrogen nuclei in $\text{Ca}(\text{OH})_2$, which was used to obtain Σr^{-6} in the calculation of the theoretical second moment as a function of the pucker parameter p . (a) A plan view projected on (0001). (b) A section projected on (1120) showing stacking of the puckered hexagonal nets of protons. Outline of unit cell is indicated by dashed lines. The open and solid circles represent protons in the upper and lower levels of each net.

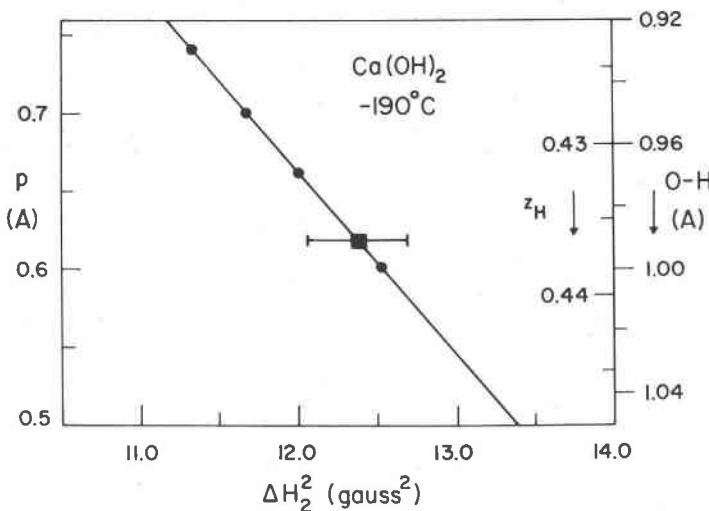


FIG. 6. Dependence of the theoretical second moment $\Delta H_2^2(\text{calc})$ upon the pucker parameter p , and the related hydrogen position parameter z_H and the O-H distance, for $\text{Ca}(\text{OH})_2$ crystal powder at -190° C. , where $a=3.585\text{ \AA}$ and $c=4.874\text{ \AA}$. The experimentally obtained average of $12.4\pm 0.3\text{ gauss}^2$ for $\Delta H_2^2(\text{exp})$ is plotted (solid square) and the 95 per cent confidence limits indicated. The solid circles represent the theoretical second moments calculated for selected values of p .

rapidly as r_{jk} becomes large. Therefore, in calculating theoretical second moments, $\Delta H_2^2(\text{calc.})$, for comparison with experiment, the terms in $\sum_{jk} kr_{jk}^{-6}$ were obtained explicitly only for neighboring protons within a radius of approximately 6 \AA . The residual contributions by more distant protons were approximated by integration, assuming the magnetic moments of the protons to be distributed uniformly and continuously over planes, each centered between the two sub-layers of a proton net.

By inspection of Fig. 5, one finds the distance r , from a proton to its three nearest neighbors, within a given net, to be much shorter than the distances to other protons in the net and to those in adjacent nets. Moreover, the dependence of r upon p is such that $dr/dp = p/r$, which shows that r changes quite rapidly with p for $p \gtrsim 0.5\text{ \AA}$. These factors combine with the $\sum_{jk} kr_{jk}^{-6}$ dependence of the second moment to make $\Delta H_2^2(\text{calc.})$ a sensitive function of p , as shown by the results plotted in Fig. 6. For the range of p covered in Fig. 6, about 90% of $\Delta H_2^2(\text{calc.})$ comes from the three nearest neighbors of each proton. This, as well as the simple geometry of the structural model for the proton positions, is why the values obtained for $\Delta H_2^2(\text{calc.})$ can be fitted by a linear equation, in particular by

$$p = 2.07 - 0.118\Delta H_2^2(\text{calc.}) \quad (10)$$

The points in the figure, and also this equation, apply to the unit cell dimensions $a=3.585 \text{ \AA}$ and $c=4.874 \text{ \AA}$ at -190° C.

However, virtually the same results were found for $\Delta H_2^2(\text{calc.})$ using the room-temperature crystal structure. The data in Table 1 indicate that thermal expansion of the unit cell is highly anisotropic, with a changing very little with temperature. The much larger change in c increases the already large distance between adjacent proton nets and produces a small fractional change in a small contribution to the theoretical second moment. Therefore, the values obtained for $\Delta H_2^2(\text{calc.})$ using the unit cell dimensions for 20° C. are only slightly smaller than those for -190° C. ; they are fitted by a linear equation the same as Eq. (10) except that the constant term is 2.06 instead of 2.07.

In comparing these results with experiment, it must be remembered that the theoretical second moment is calculated for a static model, that is, one in which the protons do not move from their equilibrium positions. Therefore, the most reliable determination of the proton positions is from the experiments at low temperatures, where the nmr line-narrowing effects of vibrational and other motions are reduced and where the proton absorption lines were stronger and more reproducible. Thus, the best, effective value for p is $0.62 \pm 0.04 \text{ \AA}$, obtained by means of Eq. (10) from the experimental second moment of $12.4 \pm 0.3 \text{ gauss}^2$ for liquid nitrogen temperatures. This value for p corresponds to $z_H = 0.437 \pm 0.004$. The errors cited here for all values are the 95 per cent confidence limits.

The O-H interatomic distance can be obtained from p , c and z_0 . Considering the low temperature case first, the value of 0.233 for z_0 (Table 1) found by Petch (1961) at room temperature does not necessarily apply here. Moreover, no determination of z_0 in Ca(OH)_2 at liquid nitrogen temperatures by x-ray diffraction has been reported. It is quite probable, however, that for large close-packed atoms such as oxygen, z_0 in layer hydroxides does not vary significantly with decrease in temperature. This seems to be borne out by the neutron diffraction measurement of z_0 in Ca(OH)_2 at 20° and -140° C. (0.2341 and 0.2346, respectively) by Busing and Levy (1957). Consequently, a value of 0.233 was assumed for z_0 at -190° C. and when combined with $c=4.874 \text{ \AA}$ and our result that $p=0.62 \pm 0.04 \text{ \AA}$, it yielded an O-H distance of $0.99 \pm 0.02 \text{ \AA}$. This is an "effective" distance in that the calculations neglect vibrational and related displacements of the oxygen and hydrogen atoms from their equilibrium positions. Nonetheless, one would expect the displacements to be small at such low temperatures; this too, seems to be borne out by Busing and Levy's neutron diffraction measurement of the 'thermal coefficients' of oxygen and hydrogen in the c direction

at 20° and -140° C. Figure 6 shows graphically the relationships among ΔH_2^2 (calc.), p , z_H , and the O-H distance at liquid nitrogen temperatures, making the foregoing assumptions. The experimental second moment is also shown.

One would not expect to obtain an accurate value of p directly from the experimental second moment at room temperature, because of the line narrowing produced by the proton motions. Furthermore, these thermal motions are probably very complex, and this discouraged us from attempting even an approximate correction for their effects. Without any such correction, the room temperature value of 10.6 ± 0.7 gauss² for the second moment leads, via Eq. (10), to an apparent value of 0.81 ± 0.08 Å for p , which corresponds to $z_H = 0.418 \pm 0.009$ and to

TABLE 2. RESULTS OBTAINED FOR Ca(OH)₂ CRYSTAL POWDER IN THIS STUDY¹

	-190° C.	25° C.
ΔH_2^2 (exp.)	12.4 ± 0.3 gauss ²	10.6 ± 0.7 gauss ²
p	0.62 ± 0.04 Å	~ 0.81 Å
z_H	0.0437 ± 0.004	~ 0.42
O-H distance	0.99 ± 0.02 Å	~ 0.91 Å

¹ 95 per cent confidence limits are indicated. No corrections have been made for the line narrowing produced by thermal motions of the protons; the line narrowing probably is important at 25° C.

an O-H distance of 0.91 ± 0.04 Å. These results, as well as those for -190° C., are summarized in Table 2. It is of interest that even the approximate value for p at room temperature suggests a contraction in the O-H distance with increase in temperature, in the interval studied. As a comparison, if the O-H distance had expanded with increase in temperature in the same proportion as the *c* cell edge (Megaw, 1933) from the value of 0.99 Å at approximately -190° C., the expected value would have been 1.00 Å at room temperatures.

The fact that the line narrowing between -190° and 25° C. is *relatively* so small indicates that the hydrogen atoms are bound to their structural sites by relatively strong forces. In turn, this implies that at -190° C. the amplitudes of the hydrogen motions and their line narrowing effects will be small (Gutowsky, *et al.*, 1954). Therefore, it is considered that the value obtained for p at -190° C. is accurate within the limits indicated. In this connection it is interesting to note the observation of Megaw (1958) that a small discontinuity in the thermal expansion of the d(001) spacings occurs just above the boiling point of nitrogen. The discontinuity may indicate a transition temperature associated with the proton motion.

DISCUSSION

In view of the large magnitude and complex form of the thermal motion of the proton near room temperatures, it is worthwhile to compare the somewhat different results obtained in the investigations of layer hydroxides by different methods. In fact, eventual determination of the detailed structural behavior of hydrogen in such minerals and artificial compounds will require the application of more than one technique.

Busing and Levy (1957) have investigated the structure of $\text{Ca}(\text{OH})_2$ by neutron diffraction at 20° C . and -140° C . They verified the essential

TABLE 3. COMPARISON OF HYDROGEN POSITIONS IN $\text{Ca}(\text{OH})_2$ AND $\text{Mg}(\text{OH})_2$
OBTAINED BY DIFFERENT METHODS

Method and substance	Room Temp.		Low Temps. ¹		Source
	z_{H}	O-H distance	z_{H}	O-H distance	
nmr $\text{Ca}(\text{OH})_2$	~ 0.42	$\sim 0.9 \text{ \AA}$	0.437 ± 0.004	$0.99 \pm 0.02 \text{ \AA}$	This study
neutron diffraction $\text{Ca}(\text{OH})_2$	0.4248 ± 0.0006	$0.936 \pm 0.003 \text{ \AA}$ ("apparent")	0.4280 ± 0.0004	$0.944 \pm 0.002 \text{ \AA}$ ("apparent")	Busing and Levy (1957)
		0.984 \AA ("true")		0.984 \AA ("true")	
x-ray diffraction $\text{Ca}(\text{OH})_2$	0.395 ± 0.008	$0.79 \pm 0.04 \text{ \AA}$			Petch (1961)
nmr $\text{Mg}(\text{OH})_2$	0.426^2	$0.98 \pm 0.02 \text{ \AA}$			Elleman and Williams (1956)

¹ Approximately -190° C , for this study and -140° C , for the investigation by Busing and Levy (1957).

² Computed from data reported by Elleman and Williams (1956).

correctness of the Bernal-Megaw model, obtained values of 0.2341 ± 0.0003 and 0.2346 ± 0.0002 for z_0 at the two temperatures respectively, determined the temperature factors for all atoms, and determined the structural positions of hydrogen (Table 3). They observed that the thermal motion of all atoms is considerably reduced at the lower temperature but that the asymmetry of the thermal motion of each remains qualitatively the same.

The asymmetry of the thermal motion of the hydrogen nuclei is especially marked, the mean square of the displacement perpendicular to the c direction being almost three times that along the c direction. The magnitude and asymmetry of the motion of the oxygen atoms, on the other hand, are relatively small so that the oxygen atoms are essentially fixed relative to the hydrogen atoms. Busing and Levy concluded that the thermal motion of the hydrogen approximates an "umbrella" shaped distribution, and that it causes the O-H bond direction

to have an appreciable average inclination from the *c* direction. They calculated that, due to the "umbrella" shaped distribution, the O-H distance along the inclined bond direction (the "true" O-H distance listed in Table 3) is 0.984 Å at both room and the low temperatures. The "apparent" O-H distance (Table 3), $c(z_0 - z_H)$, found by them corresponds to a projection of the true bond length on the *c* direction. They concluded that the apparent O-H distance increases with decreasing temperature (a relationship suggested also by our study) because the reduced thermal motion allows the O-H bond direction to approach the *c* direction. It will be noted that the "true" O-H bond length calculated by Busing and Levy (1957) is close to the O-H distance found by us at approximately -190° C. It would be interesting to have neutron diffraction determinations of the "apparent" O-H distance at temperatures above and below -190° C. in order to observe whether a discontinuity in the change of the distance with temperature occurs in that region and whether the distance approaches the calculated "true" O-H distance.

As an interesting contrast, Petch (1961) recently has reported results from a detailed *x*-ray diffraction study of the structure of portlandite at room temperature, including an investigation of the electron density associated with the hydrogen atoms (Tables 1 and 3). An earlier stage of the study (Petch and Megaw, 1954) had verified the accepted space group, unit cell and essential structure. The new study yielded data about the locations and thermal factors of the heavier atoms which agree very well with those obtained by Busing and Levy (1957). For example, the value for the oxygen position parameter was found to be $z_0 = 0.2330 \pm 0.0004$ compared with the value $z_0 = 0.2341 \pm 0.0003$ found by Busing and Levy at room temperature. Petch investigated the locations of the hydrogen positions by $(F_0 - F_e)$ synthesis, using scattering factors for singly ionized oxygen and neutral hydrogen atoms. He attributed the occurrence of a distinct peak of approximately $0.9e\text{ A}^{-2}$ at $\pm(\frac{1}{3}, \frac{2}{3}, 0.395)$ to the electron "cloud" of the hydrogen atom. This position corresponds to a distance of 0.79 ± 0.04 Å between the center of a local electron density maximum and the center of its enclosing oxygen atom. Moreover, the thermal factors for the local "cloud" were found to be symmetrical and to be considerably smaller than the value for B_z (the smaller thermal displacement) found by Busing and Levy for the proton at room temperature.

The problem, of course, is the structural significance of the location of and the thermal factors for the electron density maxima. As Petch (1961) has pointed out, an electron cloud may not be symmetrically distributed around its associated proton in an OH ion and the amplitudes of vibration of each may differ. It is possible that some of the electron

"cloud" associated with the hydrogen nucleus may be displaced toward the bond with the oxygen. Indeed, the values obtained by *x*-ray diffraction for the O-H, N-H and C-H distances between electron density maxima in other compounds are consistently shorter than the respective values obtained by neutron diffraction for the internuclear distances. However, the O-H distance of 0.79 Å reported by Petch is appreciably shorter than O-H distances obtained in other compounds by *x*-ray diffraction.

Another recent study of interest in connection with ours is the determination by nmr of the hydrogen positions in brucite by Elleman and Williams (1956). They investigated a single crystal and observed that when its *c*-axis was perpendicular to the field \mathbf{H}_0 , identical absorption lines were obtained at 60° intervals in the zone [0001]. However, the significance of their values of 1.93 ± 0.02 Å for the H-H distance and 0.98 ± 0.02 Å for the O-H distance is difficult to assess for a number of reasons. They do not seem to have considered the likelihood and effects of motional line narrowing at room temperature or of line broadening due to field modulation and saturation; their measurements were made at room temperature only and the theoretical second moment calculated from a static model in which the term $\sum r^{-6}$ was obtained for the nine nearest neighbor protons in a single puckered net. A further uncertainty arises from the fact that single crystals of brucite are actually aggregates of crystallites whose individual *c*-axes are inclined about the morphological *c*-axis as if by rotation on any one of the *a*-axes (Brindley and Ogilvie, 1952). The amount of inclination varies from crystal to crystal, and for crystals from the classical Wood's Mine locality, the source of the crystal investigated by Elleman and Williams (1956), Brindley and Ogilvie (1952) have observed inclinations ranging from a few degrees to quite considerable angles. Moreover, the effect is likely to be most pronounced in a large crystal such as that from which the piece investigated was cut. Where a large angle of inclination occurs, the theoretical second moment cannot be calculated accurately by simple substitution of the term $\sum r^{-6}$ into Eq. (4). Unless account is taken of the probability of finding a given θ_{jk} , too small a value will be found for the O-H distance.

Of the foregoing sources of error, the two most likely candidates, modulation broadening and motional narrowing, are of about the same magnitude (~ 1 and ~ 2 gauss 2 respectively) but opposite in sign. Cancellation of these two effects would lead to spectra for brucite at room temperature corresponding to the low temperature structure. It is possibly for this reason that the apparent O-H distances found in the two nmr studies are so similar, 0.98 ± 0.02 Å for brucite at room temperature

and 0.99 ± 0.02 Å for $\text{Ca}(\text{OH})_2$ at -190° C . In any case, one would expect the O-H distances to be nearly the same in the two compounds, at the same temperature, or possibly slightly larger in $\text{Mg}(\text{OH})_2$ than in $\text{Ca}(\text{OH})_2$ because of the somewhat larger polarizing power of Mg compared to Ca atoms. This supposition agrees with the experimental results because the most likely net error in the brucite analysis would give an apparent O-H distance shorter than the actual value at -190° C .

A final point of considerable interest in connection with the structural behavior of hydrogen in $\text{Ca}(\text{OH})_2$ and related compounds is the information recently obtained from high resolution infrared spectra at room and low temperatures. Mara and Sutherland (1953) found that, with polarized infrared radiation, absorption spectra from brucite at room temperature exhibited 16 bands in the $2\text{-}\mu$ to $3\text{-}\mu$ region instead of the single sharp O-H stretching band expected at 2.75μ . They concluded from this that the accepted cell, symmetry, and Bernal-Megaw arrangement for the hydrogen atoms could not be correct. Petch (Petch and Megaw, 1954) observed a similar phenomenon in portlandite but confirmed the accepted cell and symmetry by *x*-ray diffraction. Hexter and Dows (1956) then suggested that the complex spectra in the OH stretching region were combination bands due to the coupling of OH stretching vibrations with doubly degenerate OH librational motion. They suggested that the intensity of the low frequency bands should decrease at lower temperatures and the intensity of the higher frequency bands increase. Mara and Sutherland (1956), in a second study, reported that many of the bands in the OH stretching region do disappear at liquid nitrogen temperature. Busing and Morgan (1958) made a more detailed interpretation of the absorption spectra of single crystals of $\text{Ca}(\text{OH})_2$ at room and liquid nitrogen temperatures. They found good qualitative correspondence between the spectra and the results expected from a model based on the suggestions of Hexter and Dows (1956), the results of the neutron investigation of $\text{Ca}(\text{OH})_2$ (Busing and Levy, 1957), and the assumption that the librational motion is essentially harmonic. However, a number of details in the spectra could not be accounted for in terms of the model.

Thus, a reasonably good picture of the detailed structural behavior of hydrogen in trioctahedral layer hydroxides is emerging. Nonetheless, it is evident that still further work is needed to describe and explain the motions of the hydrogen at different temperatures.

ACKNOWLEDGMENTS

We are especially indebted to Dr. M. Takeda for making a number of preliminary experiments on $\text{Mg}(\text{OH})_2$ and $\text{Ca}(\text{OH})_2$ powders and for

obtaining four of the proton spectra on which this paper is based. It is also a pleasure to acknowledge the kindness of Prof. H. E. Petch in sending us (letter, April, 1956) his value for the position parameter for oxygen prior to publication as well as that of Dr. H. D. Megaw in critically reading the manuscript and making suggestions which should help to clarify certain points in the presentation of the structural interpretation. The research was supported in part by the Office of Naval Research.

REFERENCES

- AMINOFF, G. (1919) Über die Krystallstruktur des Pyrochroits. *Geol. Fören. Förh.*, **41**, 407-430.
- ANDREW, E. R. (1953) Nuclear magnetic resonance modulation correction. *Phys. Rev.* **91**, 425.
- (1955) *Nuclear Magnetic Resonance*. Cambridge Univ. Press, N. Y.
- BERNAL, J. D. AND H. D. MEGAW (1935), The function of hydrogen in intermolecular forces. *Proc. Roy. Soc. London*, **151A**, 384-420.
- BRINDLEY, G. W. AND G. J. OGILVIE (1952) The texture of single crystals of brucite. *Acta Cryst.* **5**, 412-413.
- BUSING, W. R. AND H. A. LEVY (1957) Neutron diffraction study of calcium hydroxide. *J. Chem. Phys.* **26**, 563-568.
- and H. W. Morgan (1958) Infrared spectrum of $\text{Ca}(\text{OH})_2$. *Jour. Phys. Chem.* **28**, 998-999.
- DAS, T. P. AND E. L. HAHN (1958) *Nuclear Quadrupole Resonance Spectroscopy*. Academic Press, Inc., N. Y.
- DUVAL, C. AND J. LECOMTE (1943) Quelques remarques sur les spectres d'absorption infrarouges des minéraux. *Bull. Soc. Franç. Min.* **66**, 284-292.
- ELLEMAN, D. D. AND D. WILLIAMS (1956) Proton positions in brucite crystals. *Jour. Chem. Phys.*, **25**, 742-744.
- EWALD, P. P. AND C. HERMANN, eds. (1931) *Strukturbericht 1913-1928*, Bd. I. Akademische Verlagsgesellschaft, M.B.H./Leipzig.
- GUTOWSKY, H. S. AND D. M. HENDERSON (1956) Structural studies of minerals by means of nuclear magnetic resonance (abstr.). *Geol. Soc. Am., Bull.* **67**, 1703.
- , G. B. KISTIAKOWSKY, G. E. PAKE AND E. M. PURCELL (1949) Structural investigations by means of nuclear magnetism. I. Rigid lattices. *Jour. Chem. Phys.* **17**, 972-981.
- , L. H. MEYER AND R. E. MCCLURE (1953) Apparatus for nuclear magnetic resonance. *Rev. Sci. Instr. (U.S.A.)*, **24**, 644-652.
- , G. E. PAKE AND R. BERSOHN (1954) Structural investigations by means of nuclear magnetism. III. Ammonium halides. *Jour. Chem. Phys.* **22**, 643-650.
- HENDERSON, D. M. AND H. S. GUTOWSKY (1956) A nuclear magnetic resonance determination of the position of hydrogen in $\text{Ca}(\text{OH})_2$ -portlandite (abstr.). *Geol. Soc. Am., Bull.* **67**, 1705.
- HEXTER, R. M. AND D. A. DOWS (1956) Low-frequency librations and the vibrational spectra of molecular crystals. *Jour. Chem. Phys.* **25**, 504-509.
- MARA, R. T. AND G. B. B. M. SUTHERLAND (1953) The infrared spectrum of brucite [$\text{Mg}(\text{OH})_2$]. *Jour. Opt. Soc. Am.* **43**, 1100-1102.
- (1956) Crystal structure of brucite and portlandite in relation to the infrared absorption. *Jour. Opt. Soc. Am.* **46**, 464.

- MC CALL, D. W. AND R. W. HAMMING (1959) Nuclear magnetic resonance in crystals. *Acta Cryst.* **12**, 81-86.
- MEGAW, H. D. (1933) The thermal expansion of certain crystals with layer lattices. *Proc. Roy. Soc. London*, **142A**, 198-214.
- (1958) Some empirical problems concerning atomic bonds. *Rev. Mod. Phys.* **30**, 96-99.
- PAKE, G. E. (1948) Nuclear resonance absorption in hydrated crystals; fine structure of the proton line. *Jour. Chem. Phys.* **16**, 327-336.
- (1950) Fundamentals of nuclear magnetic resonance absorption. I. *Am. J. Phys.*, **18**, 438-452; II. 473-486.
- PETCH, H. E. (1961) The hydrogen positions in portlandite, $\text{Ca}(\text{OH})_2$, as indicated by the electron distribution. *Acta Cryst.* **14**, 950-957.
- AND H. D. MEGAW (1954) Crystal structure of brucite $\text{Mg}(\text{OH})_2$ and portlandite $\text{Ca}(\text{OH})_2$ in relation to infrared absorption. *Jour. Opt. Soc. Am.*, **44**, 744-745.
- SWANSON, H. E. AND E. TATGE (1953) Standard x-ray diffraction powder patterns. *Nat. Bur. Stand. Cir.* **539**, 1, 58-59.
- VAN VLECK, J. H. (1948) The dipole broadening of magnetic resonance lines in crystals. *Phys. Rev.* **74**, 1168-1183.
- WYCKOFF, R. W. G. (1948) *Crystal Structures*, vol. 1. Interscience Publ., N. Y.
- YEOU TA (1940), Dichroisme de la brucite dans le proche infrarouge. *Comptes rendus*, **211**, 467-468.

Manuscript received, April 25, 1962.